

Total Current Blockade in an Ultra-Cold Dipolar Quantum Wire

L.H. Kristinsdóttir,¹ O. Karlström,¹ J. Bjerlin,¹ J.C. Cremon,¹ P. Schlagheck,² A. Wacker,¹ and S.M. Reimann¹

¹Mathematical Physics, LTH, Lund University, Box 118, 22100 Lund, Sweden

²Département de Physique, Université de Liège, 4000 Liège, Belgium

Cold atom systems offer a great potential for the future design of new mesoscopic quantum systems with properties that are fundamentally different from semiconductor nanostructures. Here, we investigate the *quantum-gas analogue* of a quantum wire, and find a new scenario for the quantum transport: Attractive interactions may lead to a complete suppression of current in the low-bias range, a *total current blockade*. We demonstrate this effect for the example of ultra-cold quantum gases with dipolar interactions.

The electronic Coulomb blockade in mesoscopic quantum dots has been an intensive topic of research over the last two decades. The flow of electrons through a quantum dot between two reservoirs turned out to be an extremely versatile tool for addressing a wide range of fundamental effects. Examples range from investigating the structure of electronic many-particle states [1, 2] and Kondo physics [3–5], to quantifying the spin dephasing due to coupling to nuclear degrees of freedom [6–8], or coherent effects [9].

Ultra-cold atoms in traps are very similar to quantum dots – a few quantum particles confined by a (often low-dimensional and harmonic) potential. What makes these systems particularly interesting is, that one essentially can freely engineer their properties, and even control the shape and strength of the inter-particle interactions. More recently this sparked great interest in making (quantum-)logical devices with ultra-cold atoms and molecules analogous to those in electronics and spintronics [10–15].

“Interaction blockade” as the cold-atom analog of electronic Coulomb blockade [16] was experimentally first seen in tunneling processes in optical lattices [17] and analyzed theoretically for one-dimensional triple-well systems [18]. Atom trapping with numbers down to single-atom precision was reported in a remarkable recent experiment by Serwane *et al.* [19], reaching the few-body limit with full control over confinement and inter-particle interactions. The experimental realization of *quantum transport* of cold atoms through a small quantum few-body system that is brought in contact with two large atomic reservoirs, however, has up to now posed a great experimental challenge. A first experimental breakthrough was reported recently in an experiment by Brantut *et al.* [15], that clearly demonstrates the possibility to engineer both a ballistic and a diffusive channel between two cold atom reservoirs, opening up a host of new perspectives in mesoscopic quantum physics.

Inspired by this recent experimental progress, we study in this Letter the quantum transport through wire-like confinement of a few ultra-cold fermions. In the framework of the experiment by Brantut *et al.* [15], such a structure could be realized by two optical barriers within

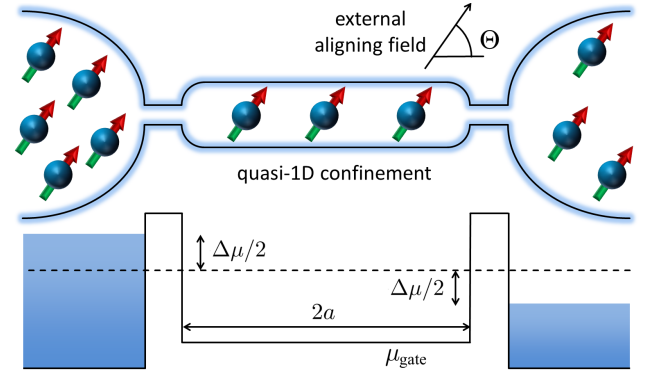


Figure 1. Upper panel: Schematic figure of the system. Lower panel: Sketch of the setup in analogy to the case of mesoscopic conductors. Two reservoirs with a degenerate gas of ultra-cold spin-half dipolar particles are connected via a quasi one-dimensional structure, a “wire” of length $2a$. The difference in chemical potential between the reservoirs, $\Delta\mu$, creates a particle current if the dipoles can be added and removed from the wire. Levels in the wire can be tuned by a gate potential, μ_{gate} . The interaction between the particles in the wire can be varied by the tilt angle of the dipoles, Θ , and allows to observe significantly different current patterns.

the channel, created by focusing two blue-detuned laser beams perpendicularly onto the channel.

A particularly interesting aspect of studying transport with cold atoms or molecules is the tunability of the interactions between the particles - often being of contact type, and experimentally controlled by Feshbach resonances. Here, we choose to study fermions with electric dipolar interactions which can be controlled by an external field [20]. Changing the interactions from repulsive to attractive, we report the occurrence of *total current blockade*, where the attractive interaction hinders transport for finite biases independent of the gate potential. While the total current blockade would also occur with attractive contact interactions, dipolar interactions also make it possible to study localization effects due to the long-range nature of the force, in much analogy to electrons in quantum wires [21].

The setup of the system described above is sketched in Fig. 1. Similar to the recent study by Brantut *et*

al. [15], two fermionic reservoirs with controllable difference in chemical potential $\Delta\mu$ are connected by a quasi one-dimensional trap. In this region, the potential energy of the particles can be varied by the parameter μ_{gate} in full analogy to electrons in gated semiconductor nanostructures. The electric dipole moment p of the particles can be orientated along an external field by a tilt angle Θ with respect to the z axis along the quasi one-dimensional channel (see Fig. 1). One can thereby also minimize the dipolar component of the particle interactions in the leads, and stabilize the dipolar gas against collapse in the left and right reservoirs, required to be two-dimensional and appropriately oriented with respect to the external field. A small local variation of the orientation angle Θ allows inducing attractive or repulsive interactions locally within the wire.

Model.—The interaction between two dipoles with distance r and angle θ_{rd} between the dipole orientation and particle separation is generally given by [22, 23]

$$V_{\text{dd}} = \frac{d^2}{r^3} (1 - 3 \cos^2 \theta_{rd}) \Big|_{r>0} - \frac{4\pi}{3} C d^2 \delta^3(\mathbf{r}) \quad (1)$$

The coupling strength is $d^2 = p^2/(4\pi\epsilon_0)$, where p is the dipole moment strength, ϵ_0 is the vacuum permittivity and $C = 1$. (For magnetic dipoles, $d^2 = \mu_0\mu^2/(4\pi)$ is significantly smaller, where μ_0 is the vacuum permeability, μ the magnetic moment and $C = -2$.) While the first term provides the common angular dependence of dipole-dipole interaction, the second term provides a contact interaction which is frequently disregarded. Within the quantum wire, the dipoles are confined in x and y by a two-dimensional harmonic oscillator of characteristic length l_{\perp} , rendering a quasi one-dimensional system in the z -direction for small l_{\perp} . Integrating over the lateral x and y degrees of freedom one arrives at an effective one-dimensional dipole-dipole interaction

$$V_{\text{dd}}^{\text{eff}}(z_1, z_2) = U_{\text{dd}}(\Theta) f\left(\frac{|z_1 - z_2|}{l_{\perp}}\right) + \frac{2C d^2}{3l_{\perp}^2} \delta(z_1 - z_2) \quad (2)$$

with $f(u) = -2u + \sqrt{2\pi}(1 + u^2)e^{u^2/2} \text{erfc}(u/\sqrt{2})$ where erfc is the complementary error function [24]. The interaction coefficient

$$U_{\text{dd}} = -\frac{d^2[1 + 3 \cos(2\Theta)]}{8l_{\perp}^3}, \quad (3)$$

can be either positive or negative depending on the dipole tilt angle Θ . If the dipoles are aligned in the z direction ($\Theta = 0^\circ$) they attract each other, $U_{\text{dd}} < 0$, while they repel one another, $U_{\text{dd}} > 0$, if they are orientated perpendicular to the z direction ($\Theta = 90^\circ$). For an intermediate angle ($\Theta_{\text{crit}} \simeq 54.7^\circ$) this long-range part of the dipole interaction vanishes.

In the z -direction the wire is modeled as a finite square well (see Fig. 1) of width $2a$ and barrier height V_0 . Ap-

plying the single-particle basis of eigenstates for this potential well, the configuration interaction method (exact diagonalization) is used to find the lowest energy states of $N = 1$ to $N = 6$ dipoles in the quantum wire. Here the dipolar particles are assumed to be spin-half fermions. In the following we use $d^2 = \hbar^2 a/m$, $l_{\perp} = 0.14a$, and $V_0 = 300\hbar^2/ma^2$. (For RbK molecules with $p = 0.57$ Debye [25] this corresponds to $a \simeq 0.6\mu\text{m}$ and an energy unit of $\hbar^2/ma^2 \simeq k_B 10\text{nK}$)

Transitions between states of different N occur due to particle exchange with the reservoirs, as described by rates $\Gamma_{a \rightarrow b}$ evaluated by Fermi's golden rule. The corresponding matrix elements between the many particle state are evaluated following the work of [26, 27] for mesoscopic electronic systems. Assuming, that the occupations of the single-particle states in the particle reservoirs are given by Fermi-functions with $k_B T = 0.02\hbar^2/ma^2$, this provides a Pauli master equation for the probabilities of the different many-particle states in the confinement region. For the stationary state we obtain the (particle) current \dot{N} between the reservoirs and the (differential) conductance $G = d\dot{N}/d\Delta\mu$.

Main results.—First we neglect the contact term of the dipolar interaction, which can be eliminated by Feshbach resonances [28], and obtain the conductance diagrams displayed in Fig. 2. For repulsive interaction between the dipoles, see Figs. 2(a)-(b), the conductance diagrams resemble those of Coulomb blockade as intensively studied by electron transport in mesoscopic structures [1].

In the diamond-shaped regions of vanishing conductance, the particle number N in the wire is fixed, and the current between the reservoirs is strongly suppressed. At the borders between the N and $(N + 1)$ -particle region, conductance is possible due to single-particle transitions. This scenario does not depend on the specific form of the (repulsive) interaction [16, 17].

In contrast to electronic systems, however, the tunability of the interaction for dipolar fermions allows to reduce the interaction strength (Figs. 2(c)-(d)) and even reach a scenario where the interactions become attractive, see Fig. 2(e): We then obtain a total current blockade at low detuning $\Delta\mu$ independent of the gate potential μ_{gate} . This is a clear-cut signature of attractive interactions.

The total current blockade is associated with the vanishing of the diamonds for odd N . This can be understood by the two-fold degeneracy of the single particle levels due to the particle spin: The first particle enters the system at the level energy, while the second particle experiences an additional interaction energy U between the spin-degenerate particles in a level. The single occupancy of the level, i.e. a state with odd N , is stable if the reservoirs allow for adding the first particle, but not the second. For $U > 0$ (i.e. the conventional repulsive Coulomb interaction or $\Theta > 54.7^\circ$ for the dipoles studied here) this is possible. Thus, the blockade diamonds with an odd number of particles N and lines of finite conduct-

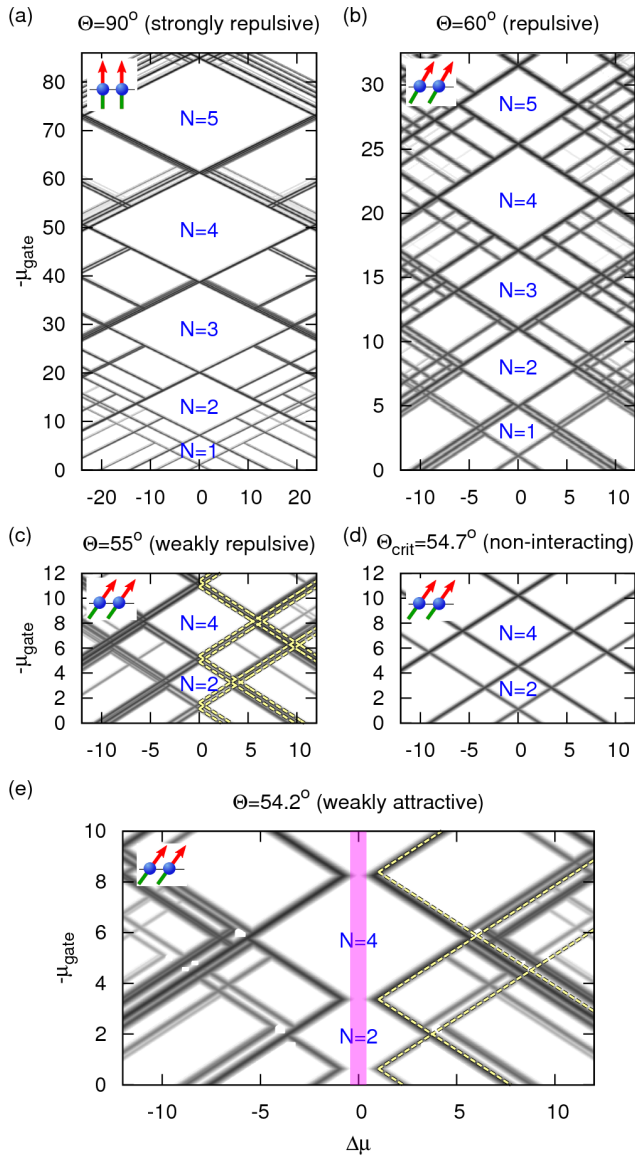


Figure 2. Conductance between the particle reservoirs as a function of reservoir potential difference $\Delta\mu$ and gate potential μ_{gate} . Here the contact part of the dipolar interaction is neglected and the long-range part, which can be tuned by the angle Θ of the external field, changes from (a) strongly repulsive, via (d) non-interacting, to (e) the weakly attractive case. The region of total current blockade for attractive interaction is colored in magenta in (e). The dashed (yellow) lines in (c) and (e) indicate the results of a simplified quasi-independent-particle model. The calculations were performed for $d^2 = 1.0 \hbar^2 a/m$ and $l_{\perp} = 0.14a$. The μ -scale is in units of \hbar^2/ma^2 . Note the different scales in panel (a) and (e).

ance at the separation to the blockade diamonds with even N appear in Figs. 2(a),(b). With decreasing interaction the width of all diamonds shrinks and the width of the odd- N diamonds vanishes at $U = 0$ as can be seen in Fig. 2(d). Now, for negative U the situation of a single fermion in a level is unstable as it attracts a particle

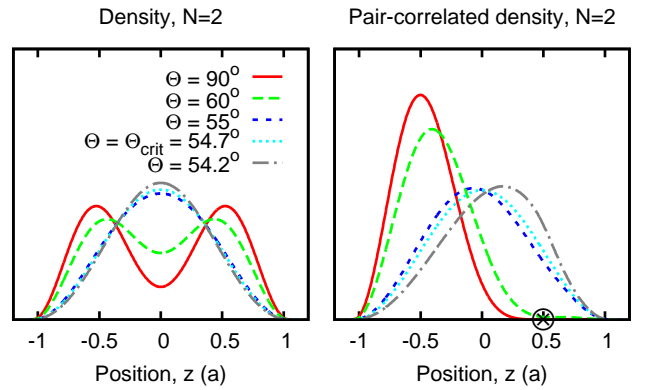


Figure 3. Particle density (left) and pair-correlation function (right) for $N = 2$ particles at the tilt angles Θ used in Fig. 2(a)-(e). For the pair-correlation function one particle is fixed at the position marked with the symbol \otimes . As the interaction goes from strongly repulsive ($\Theta = 90^\circ$) to weakly attractive ($\Theta = 54.2^\circ$) the two particles evolve from a localized state to a delocalized state with a slight tendency to clustering.

with the opposite spin. This instability does not allow for configurations with odd N for low $\Delta\mu$. Therefore, single-particle transitions between the reservoir and the wire are excluded, resulting in the absence of current flow in the region of total current blockade, see the magenta shaded area in Fig. 2(e). (The case of two-particle transitions is addressed below.)

For weak interactions, this can be quantified by a quasi-independent-particle model: The single-particle level energies of the quantum well are approximated by $n^2 E_1$ where $n = 1, 2, \dots$ and E_1 is the single-particle ground state energy. Using the analytic eigenfunction of the infinite well, we approximate the interaction energy by first order perturbation theory. Then the energy difference between the $N + 1$ and the N -particle ground state is given by

$$\mu_{N+1} = \mu_{\text{gate}} + (n+1)^2 E_1 + \left(\frac{2}{3}n + \delta\right) U \quad (4)$$

where $U \equiv 3l_{\perp} U_{\text{dd}}/a$ and μ_{gate} is the gate potential relative to the bottom of the well. Here, $n = N/2$ and $\delta = 0$ for even N while $n = (N-1)/2$ and $\delta = 1$ for odd N . The lines of the diamonds are given by the crossing points of μ_{N+1} with the chemical potential $\pm\Delta\mu/2$ in the left or right reservoir, respectively. The corresponding dashed (yellow) lines shown in Figs. 2(c,e) agree well with the main conductance lines obtained from the full many-particle calculation. Thus, correlations do not play any essential role here.

In contrast, such an approach does not hold for stronger interaction strengths. Here the many-particle states show strong localization effects as shown in Fig. 3 for the two-particle states. For $\Theta = 90^\circ$ and to a smaller extent for $\Theta = 60^\circ$, one observes two peaks in

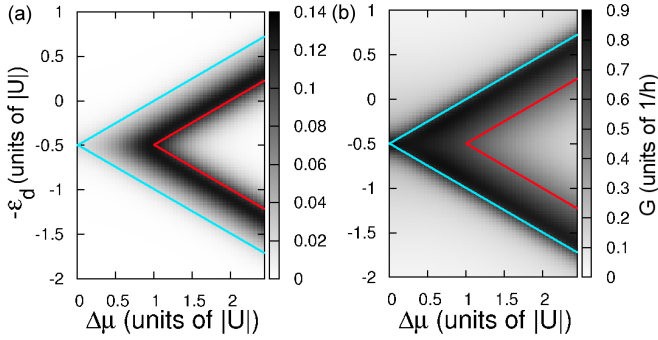


Figure 4. Conductance through a single spin-degenerate level at energy ε_d for the case of inter-particle attraction, resulting in negative charging energy $U < 0$. The temperature is $k_B T = |U|/10$, and the couplings are $\Gamma_L = \Gamma_R = |U|/50$ for (a), and $\Gamma_L = \Gamma_R = |U|/4$ for (b). The red and blue lines show the onset of sequential and pair-tunneling, respectively.

the particle density (left panel), and the pair-correlation function (right panel) shows that the probability to find the two particles within the same peak is strongly reduced. This is the scenario of Wigner localization as very recently studied theoretically for cold polar molecules in [29]. In full analogy to mesoscopic electron conduction [21], signatures of this localization can be clearly detected in the conductance plots Fig. 2(a)-(b) where several, almost degenerate lines are observed on the top of the diamonds, which result from spin excitations of the localized particles.

We note that this scenario of Wigner localization would not arise in transport processes with atomic species that only interact through a contact interaction potential.

Improved interaction model.—For attractive interaction ($\Theta = 54.2^\circ$), the pair-correlation function is shifted to the right, see the right panel of Fig. 3, *i.e.* the probability to find both fermions on the same spot is enhanced for the groundstate. In this case the contact interaction in Eq. (2) becomes relevant. Taking this term into account provides some modifications of the scenario depicted in Fig. 2, while the main features remain. For the case of electric dipoles, the contact interaction is repulsive and compensates a part of the long-range attraction, so that smaller angles Θ are required to observe the vanishing of the diamonds with odd N . Furthermore, since the particle density increases with the number of particles N , the contact interaction becomes more relevant for higher N , and thus smaller angles are required for the vanishing of diamonds with higher N . We have observed this for e.g. $\Theta = 46^\circ$, where the $N = 1$ diamond has already vanished, while the $N = 3$ diamond is very small and the $N = 5$ diamond is still well established. In this case the total current blockade due to the attractive interaction extends only over a part of the spectrum.

Pair-tunneling.—As discussed above, the situation of a single fermion in a level is unstable for the case of at-

tracting particles, $U < 0$. Thus, single-particle transitions between the reservoir and the wire are excluded for sufficiently low values of temperature and bias $\Delta\mu$. Here we want to illuminate the role of two-particle transitions, which may occur due to higher-order processes in the coupling between the reservoirs and the wire [30, 31].

There are two kinds of processes: Normal co-tunneling, which results in a weak background conductance for any bias, and pair-tunneling which, neglecting the effects of temperature and lifetime broadening, is only allowed for $|E_{2n+2} - E_{2n}| < \Delta\mu$, where E_N is the ground state energy of the N -particle state and n is an integer. When present, pair-tunneling gives a more pronounced contribution than co-tunneling [30]. Being of second order, these processes scale as Γ^2 , where Γ is the single particle transition rate. Thus, for sufficiently weak couplings they can be neglected compared to sequential single-particle tunneling.

Figure 4 shows the differential conductance of a single spin-degenerate level with $U < 0$, calculated by the second order von Neumann formalism [26, 32]. For weak contact coupling, Fig. 4(a) displays only a small conductance at low values of $\Delta\mu$. This can be attributed to a weak pair-tunneling background and to the temperature broadening $\sim 3k_B T$ of the direct tunneling peaks at $\varepsilon_d = -U/2 \pm (\Delta\mu + U)/2$ for $\Delta\mu > -U$, which correspond to the red lines in Fig. 4. This demonstrates that the total blockade of conductance is verified for $\Gamma \ll k_B T \ll |U|$, as is the case in Fig. 2(e).

On the other hand, one has to keep in mind that, as Γ approaches U , pair-tunneling becomes energetically allowed. Hence, we observe the onset of conduction along the blue lines $|E_2 - E_0| = \Delta\mu$ in Fig. 4(b). (In our case $E_2 = 2\varepsilon_d + U$ and $E_0 = 0$.) Normal co-tunneling can also be observed as a weak background present at all $\Delta\mu$ and ε_d . Thus, the total blockade of conductance does not persist at strong couplings between the wire and the reservoirs. For even higher couplings, our model fails and Kondo-like effects become important [33]. This shows that the energy barriers confining the wire cannot be arbitrarily weak for the observation of the total current blockade, as otherwise pair-tunneling masks the scenario.

Experimental challenges.—From the experimental point of view, measuring a weak atomic current in a mesoscopic transport process appears challenging. In the experimental studies of quantum transport through atom traps by Brantut *et al.* [15], the integrated current is measured by a sensitive detection of population differences in the reservoirs. This opens up a new field of mesoscopic physics research. Complementary experimental information on the atomic current could, for instance, be inferred from a time-of-flight absorption image that renders the momentum distribution of the transported atoms. As an alternative, a stimulated Raman adiabatic passage (STIRAP) of the atoms could be induced by irra-

diating the transport region with two spatially displaced laser beams (see, e.g., Ref. [34]). An atom that propagates through this irradiated region would then necessarily transfer a photon from one of the laser beams to the other, while an atom that propagates in the opposite direction would revert this photon transfer. A careful measurement of the net photon transfer between the beams after a suitable evolution time would then give rise to the integrated atomic net current across the atom-photon interaction region. We remark that standard techniques to detect individual atoms using fluorescence imaging [35, 36] or electron beams [37] would not work in this context as they do not distinguish between left-moving and right-moving atoms.

Conclusions.—We have shown that dipolar quantum gases allow for the observation of a total current blockade for small differences in chemical potentials between the reservoirs. In this context the often neglected contact interaction part of the dipole-dipole interaction turns out to repress the onset of total current blockade.

From the experimental side, studies of quantum transport with ultra-cold atoms and the many-body effects of interaction blockade are still in their infancy. Here, we highlighted the prospects for the specific example of a few-body system with dipolar interactions between the confined atoms. We demonstrated the possibilities offered by the tunability of the dipole-dipole interaction in a quasi one-dimensional geometry by an external field.

We thank the Swedish Research Council and the Nanometer Structure Consortium at Lund University (nmC@LU) for financial support. Furthermore, we thank Georg Bruun, Frank Deuretzbacher, Georgios Kavoulakis and Chris Pethick for discussions regarding the dipolar interaction potential.

-
- [1] S. M. Reimann and M. Manninen, *Rev. Mod. Phys.* **74**, 1283 (2002)
- [2] R. Hanson, L. P. Kouwenhoven, J. R. Petta, S. Tarucha, and L. M. K. Vandersypen, *Rev. Mod. Phys.* **79**, 1217 (2007)
- [3] L. I. Glazman and M. E. Raikh, *JETP Lett.* **47**, 452 (1988)
- [4] T. K. Ng and P. A. Lee, *Phys. Rev. Lett.* **61**, 1768 (1988)
- [5] D. Goldhaber-Gordon, H. Shtrikman, D. Mahalu, D. Abusch-Magder, U. Meirav, and M. A. Kastner, *Nature* **391**, 156 (1998)
- [6] J. R. Petta, A. C. Johnson, J. M. Taylor, E. A. Laird, A. Yacoby, M. D. Lukin, C. M. Marcus, M. P. Hanson, and A. C. Gossard, *Science* **309**, 2180 (2005)
- [7] F. H. L. Koppens, J. A. Folk, J. M. Elzerman, R. Hanson, L. H. W. van Beveren, I. T. Vink, H. P. Tranitz, W. Wegscheider, L. P. Kouwenhoven, and L. M. K. Vandersypen, *Science* **309**, 1346 (2005)
- [8] F. H. L. Koppens, C. Buizert, K. J. Tielrooij, I. T. Vink, K. C. Nowack, T. Meunier, L. P. Kouwenhoven, and L. M. K. Vandersypen, *Nature* **442**, 766 (2006)
- [9] H. A. Nilsson, O. Karlström, M. Larsson, P. Caroff, J. N. Pedersen, L. Samuelson, A. Wacker, L.-E. Wernersson, and H. Q. Xu, *Phys. Rev. Lett.* **104**, 186804 (2010)
- [10] B. Seaman, M. Krämer, D. Anderson, and M. Holland, *Phys. Rev. A* **75**, 023615 (2007)
- [11] R. Pepino, J. Cooper, D. Anderson, and M. Holland, *Phys. Rev. Lett.* **103**, 140405 (2009)
- [12] R. Pepino, J. Cooper, D. Meiser, D. Anderson, and M. Holland, *Phys. Rev. A* **82**, 013640 (2010)
- [13] Y. Qian, M. Gong, and C. Zhang, *Phys. Rev. A* **84**, 013608 (2011)
- [14] M. Bruderer and W. Belzig, *Phys. Rev. A* **85**, 13623 (2012)
- [15] J.-P. Brantut, J. Meineke, D. Stadler, S. Krinner, and T. Esslinger, *Science* **337**, 1069 (2012)
- [16] K. Capelle, M. Borgh, K. Kärkkäinen, and S. M. Reimann, *Phys. Rev. Lett.* **99**, 010402 (2007)
- [17] P. Cheinet, S. Trotzky, M. Feld, U. Schnorrberger, M. Moreno-Cardoner, S. Fölling, and I. Bloch, *Phys. Rev. Lett.* **101**, 090404 (2008)
- [18] P. Schlagheck, F. Malet, J. C. Cremon, and S. M. Reimann, *New J. Phys.* **12**, 065020 (2010)
- [19] A. Serwane, G. Zuern, T. Lompe, T. Ottenstein, A. Wenz, and S. Jochim, *Science* **332**, 336 (2011)
- [20] T. Lahaye, C. Menotti, L. Santos, M. Lewenstein, and T. Pfau, *Rep. Prog. Phys.* **72**, 126401 (2009)
- [21] L. H. Kristinsdóttir, J. C. Cremon, H. A. Nilsson, H. Q. Xu, L. Samuelson, H. Linke, A. Wacker, and S. M. Reimann, *Phys. Rev. B* **83**, 041101 (2011)
- [22] J. D. Jackson, *Classical Electrodynamics*, 3rd ed. (John Wiley & Sons, New York, 1998)
- [23] R. Skinner and J. A. Weil, *Am. J. Phys.* **57**, 777 (1989)
- [24] F. Deuretzbacher, J. C. Cremon, and S. M. Reimann, *Phys. Rev. A* **81**, 063616 (2010)
- [25] K.-K. Ni, S. Ospelkaus, D. Wang, G. Quéméner, B. Neyenhuis, M. de Miranda, J. Bohn, and D. Jin, *Nature* **464**, 08953 (2010)
- [26] J. N. Pedersen and A. Wacker, *Phys. Rev. B* **72**, 195330 (2005)
- [27] F. Cavaliere, U. D. Giovannini, M. Sassetti, and B. Kramer, *New J. Phys.* **11**, 123004 (2009)
- [28] J. Werner, A. Griesmaier, S. Hensler, J. Stuhler, and T. Pfau, *Phys. Rev. Lett.* **94**, 183201 (2005)
- [29] M. Knap, E. Berg, M. Ganahl, and E. Demler, *Phys. Rev. B* **86**, 064501 (2012)
- [30] J. Koch, M. E. Raikh, and F. von Oppen, *Phys. Rev. Lett.* **96**, 056803 (2006)
- [31] M.-J. Hwang, M.-S. Choi, and R. López, *Phys. Rev. B* **76**, 165312 (2007)
- [32] J. N. Pedersen and A. Wacker, *Physica E* **42**, 595 (2010)
- [33] J. Koch, E. Sela, Y. Oreg, and F. von Oppen, *Phys. Rev. B* **75**, 195402 (2007)
- [34] A. Kuhn, M. Hennrich, and G. Rempe, *Phys. Rev. Lett.* **89**, 067901 (2002)
- [35] W. S. Bakr, A. Peng, M. E. Tai, R. Ma, J. Simon, J. I. Gillen, S. Fölling, L. Pollet, and M. Greiner, *Science* **329**, 547 (2010)
- [36] J. F. Sherson, C. Weitenberg, M. Endres, M. Cheneau, I. Bloch, and S. Kuhr, *Nature* **467**, 67 (2010)
- [37] P. Würtz, T. Langen, T. Gericke, A. Koglbauer, and H. Ott, *Phys. Rev. Lett.* **103**, 080404 (2009)